Front. Phys. 13(4), 137802 (2018)
https://doi.org/10.1007/s11467-018-0768-0

RESEARCH ARTICLE

Quantum confinement effect in β-SiC nanowires

Gang Peng (彭刚)[1,†], **Xiaoyan Yu** (于晓燕)[2], **Yan-Lan He** (何焰兰)[1], **Gong-Yi Li** (李公义)[1], **Yi-Xing Liu** (刘一星)[1], **Xinfang Zhang** (张鑫方)[1], **Xue-Ao Zhang** (张学骜)[1]

[1] *college of Science, National University of Defense Technology, Changsha* 410073, *China*
[2] *School of Electronic & Communication Engineering, Guiyang University, Guiyang* 550005, *China*
Corresponding author. E-mail: [†]*penggang@nudt.edu.cn*
Received August 23, 2017; accepted January 5, 2018

The quantum confinement effect is important in nanoelectronics and optoelectronics applications; however, there is a discrepancy between the theory of quantum confinement, which indicates that band-gap widening occurs only at small sizes, and experimental observations of band-gap widening in large-diameter nanowires (NWs). This paper reports an obvious blue shift of the absorption edge in the UV-visible absorption spectra of SiC NWs with diameters of 50–300 nm. On the basis of quantum confinement theory and high-resolution transmission electron microscopy images of SiC NWs, band-gap widening in SiC NWs with diameters of up to hundreds of nanometers is fully explained; the results could help to explain similar band-gap widening in other NWs with large diameters.

Keywords quantum confinement effect, SiC nanowires (SiC NWs), band gap

PACS numbers 03.65.Sq, 78.67.-n

1 Introduction

Band-gap widening in nanostructured semiconductor materials has been studied for 30 years [1, 2]. Many models have been proposed to explain the phenomenon; the most important are quantum confinement [3–5], surface states [6–8], and defect states [9]. Quantum confinement can be observed when the diameter of a material is of the same magnitude as the de Broglie wavelength of the electron wave function. Along with quantum effects, surface effects become more significant when the nanocrystal size is decreased to approximately 1 nm because of the resulting rapid increase in the surface atom ratio. In addition, defect states including point defects, line imperfections, face defects, and body defects arising during the growth process will result in redistribution of the charge and internal stress; thus, the band gap will be altered. To date, the commonly accepted theory is that the band gap is widened as a result of quantum confinement for crystallite sizes at which the diameter of a material is of the same magnitude as the de Broglie wavelength of the electron wave function [10–12]. When materials are that small, their electronic and optical properties deviate substantially from those of bulk materials [13]. As a result, the band gap becomes size-dependent, which ultimately results in a blue shift in light emission (or absorption) as the particle size decreases. Wu *et al.* [5] found the first experimental evidence of the quantum confinement effect in β-SiC nanocrystallites, which were fabricated by electrochemical etching of a polycrystalline β-SiC target and had sizes of 1–6 nm. The photoluminescence and photoluminescence excitation spectra, in which the emission band maximum ranged from 440 to 560 nm, showed clear evidence of quantum confinement in β-SiC nanocrystallites. Then Wang *et al.* [14] studied the quantum confinement effect in SiC nanostructures using density functional theory (DFT) and the local-density approximation (LDA) approach. They found that the band gaps of SiC nanowires (NWs) and SiC nanodots decreased with increasing diameter d of the nanostructures from 0.5 to 2 nm owing to the quantum confinement effect, and the band gap (E_g) could be fitted using $E_g = E_g^{bulk} + 0.51d^{-1.245}$ for SiC NWs and $E_g = E_g^{bulk} + 2.18d^{-0.85}$ for SiC nanodots, where E_g^{bulk} is the band-gap value of bulk SiC. However, many experimental studies also found an obvious increase in the band-gap energy of nanowires with diameters of up to 300 nm [15–17]. For example, Luo *et al.* [15] studied NWs and nanobelts of SnO_2 with a diameter of approximately 300 nm and found a band gap of 3.74 eV for the NWs and 3.81 eV for the nanobelts, both of which were larger than the value of 3.62 eV for bulk SnO_2. Eskizeybek *et al.* [16] studied the diameters of spherical or irregular CdO nanoparticles ranging in size from 20 to 50 nm; UV-visible spectroscopy analysis of these particles

showed that the direct gap of the CdO NWs was approximately 2.60 eV, which was higher than that of bulk CdO (2.3 eV). Phuruangrat *et al.* [17] recently pointed out that the UV-visible absorption edge of CdS NWs with diameters of approximately 100 nm showed a blue shift, which was also explained by the quantum confinement effect. All the above studies attributed the band-gap widening to the quantum confinement effect but did not present an explanation. As we know, theoretical calculations suggest that such effects should not be observed because the diameter of the investigated NWs is as high as hundreds of nanometers, which is much larger than the de Broglie wavelength.

To explore the unexpected existence of the quantum confinement effect in NWs with large diameters, we studied SiC NWs in this work because SiC is an important wide-band-gap semiconductor with superior properties, such as a high breakdown field strength, high thermal conductivity, and high saturation drift velocity [18, 19]. Moreover, it is important that SiC NWs have excellent physical and chemical stability even at sizes of a few nanometers. This study was designed in three phases. In the first phase, the band gap as a function of the diameter of β-SiC NWs was calculated by Brus's band-gap widening equation under the effective-mass approximation [1]. The calculation results showed that only β-SiC NWs with diameters of less than 6 nm would exhibit a strong quantum confinement effect. In the second phase, SiC NWs with diameters of approximately 50–300 nm were prepared and proven to be β-SiC by X-ray diffraction (XRD) analysis. Then the UV-visible spectra were measured, and the absorption edge was found to be obviously larger than the band gap of the bulk β-SiC crystal. In the third phase, to explore these contradictory findings, high-resolution transmission electron microscopy (HRTEM) images of SiC NWs were studied. The images indicated that the SiC NWs were made up of nanosheets with thicknesses of 1–5 nm, which was the reason for the obvious blue shift of the absorption edge. This work could fully explain the band-gap widening of SiC NWs with diameters of up to hundreds of nanometers and similar phenomena in other NWs with large diameters. Moreover, the insight obtained from this work could be employed to explain the strain effect (which changes the dimension of the lattice size) on the energy bands of SiC NWs [20, 21], which leads to several interesting effects such as piezoresistance.

2 Calculation of band gap as function of diameter

In a previous report, Wang *et al.* [14] obtained the band gap (E_g) as a function of the SiC NW diameter for diameters of 0.5–2 nm by fitting four data points calculated on the basis of DFT using the LDA approach, that is, $E_g = E_g^{bulk} + 0.51d^{-1.245}$. However, we considered that this equation was not a universal formula because it is not based on a physical perspective, and the number of fitting points was only four. Brus [1] studied the band gap in semiconductor crystallites with sizes of $\sim$ 15 Å to several hundred angstroms using experiments and theory. The nanocrystallites were treated as clusters because they were too small to have bulk-like electronic wave functions, even though they exhibited bulk-like crystal structure. The cluster molecular orbital (MO) could be obtained from the infinite crystal Bloch MO by ignoring the weak wave vector k dependence of site x. Thus, the added energy of an extra electron (hole) in a tiny crystallite could be treated as the quantum localization energy of a pseudo-electron (pseudo-hole) with effective mass m_e (m_h), assuming that the cluster has a compact shape with a center of symmetry in k space, and the effective mass constant m_e (m_h) was used instead of the effective mass tensor. Furthermore, it is recommended to add the electron–hole correlation, in a certain special sense, to the polarization energy terms because the term for the Coulomb interaction in the presence of the crystallite surface should be considered. Further, the polarization terms are assumed to follow the standard solid-state ansatz, in which the electron and hole interact with each other via a shielded Coulomb interaction. Finally, the band-gap energy is [1]

$$E_g \approx E_g^{bulk} + \frac{\hbar^2\pi^2}{2R^2}\left(\frac{1}{m_e}+\frac{1}{m_h}\right) - \frac{1.8e^2}{4\pi\varepsilon_0\varepsilon_r R}, \qquad (1)$$

where R is the particle size, e is the electron charge, ε_0 is the permittivity of vacuum, and ε_r is the dielectric constant. The second term on the right-hand side is the quantum confinement term, which shifts E_g to a higher energy as R^{-2}, and the third term is a Coulomb term that shifts E_g to lower energy as R^{-1}. Thus, the apparent band gap would always increase when R was small enough.

To calculate the numerical relationship between the band gap of β-SiC NWs and the diameter d ($d \equiv 2R$), the related physical parameters should be obtained first. For β-SiC NWs [5], the longitudinal and transverse effective electron masses are $m_l^e = 0.647m_0$ and $m_t^e = 0.24m_0$, and the effective masses of heavy and light holes are $m_h^h = 1.2m_0$ and $m_l^h = 0.125m_0$, respectively, where m_0 is the electron rest mass [22]. In an approximate calculation [5], we took the effective mass of electrons, $m_e = \sqrt{m_l^e m_t^e} = 0.394m_0$, and that of holes, $m_h = \sqrt{m_h^h m_l^h} = 0.387m_0$, and we took the band gap of bulk β-SiC as 2.30 eV and the dielectric constant ε_r as approximately 10. Therefore, the band gap of β-SiC NWs

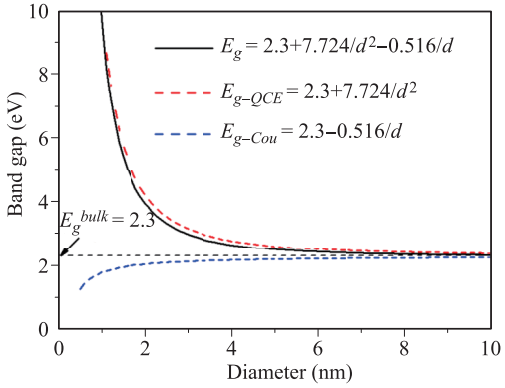

Fig. 1 Band gap of β-SiC NWs as a function of diameter. E_{g-QCE} is the band gap obtained using only the quantum confinement term, and E_{g-Cou} is the band gap obtained using only the Coulomb interaction term.

as a function of diameter is

$$E_g \approx 2.30 + \frac{7.724}{d^2} - \frac{0.516}{d}. \quad (2)$$

The band gap of β-SiC NWs as a function of diameter d is shown in Fig. 1 (black line). No adjustable parameters were used in the calculations. The figure shows that the quantum confinement term shifted E_g to higher energy as R^{-2} (red line), and the Coulomb term shifted E_g to lower energy as R^{-1} (blue line). Thus, the band gap would always increase with decreasing diameter for small NWs. Moreover, only β-SiC NWs with diameters of less than 6 nm would exhibit an obvious band-gap widening effect. This simple description should be regarded as only a first approximation of quantum confinement in semiconductors; as the dimension of the nanostructures becomes very small, this relationship could be expected to break down.

3 Experimental observation of band-gap widening in SiC NWs

β-SiC NWs with diameters of approximately 50–300 nm and lengths of approximately 0.5 mm were synthesized by pyrolyzing liquid polysilacarbosilance (l-PS) at 1300°C for 1 h by a chemical vapor deposition route [23–25]. The SiC NWs were collected from the ceramic boat [Fig. 2(a)] and rinsed sequentially in concentrated sulfuric acid (1.8 N), deionized water (18.25 MΩ·cm), sodium hydroxide (2.0 N), deionized water (18.25 MΩ·cm), dilute hydrofluoric acid (1.8 N), anhydrous alcohol, and deionized water (18.25 MΩ·cm) to remove all the raw materials, impurities, and the co-axial silicon dioxide layer. The SiC NWs were then dried in an oven before the measurements were made.

The SiC NWs were characterized using an X-ray diffractometer (Siemens D500, $\lambda = 0.1541$ nm) to determine their composition. The diffraction peaks of the SiC NWs [Fig. 2(d)] were in good agreement with the established values (JCPDS Card No. 73-1665), indicating that the NWs were well-crystallized β-SiC (cubic 3C type) [23, 26]. Then, a scanning electron microscope (SEM, Hitachi S-4800) was used to observe the morphology of the β-SiC NWs. The resulting images showed that the product consisted of β-SiC NWs with diameters ranging from 50 to 300 nm [Figs. 2(b) and (c)].

To characterize the band gap of the SiC NWs, a Hitachi UV-4100 Spec UV spectrophotometer was used to measure the UV-visible spectra from 200 to 800 nm of the as-prepared NWs collected from the ceramic boat at room temperature in air. The UV-visible absorption spectrum of the β-SiC NWs, as shown in Fig. 3, indicated that the absorption edge was approximately 465 nm. The band gap (E_g) of the bulk β-SiC was approximately 2.30 eV, from which we could calculate the corresponding absorption edge, which was 539 nm, as follows:

$$\lambda = \frac{\hbar c}{2\pi E_g}, \quad (3)$$

where $\hbar$ is the reduced Planck constant (1.05×10^{-34} J·s), and c is light velocity (299, 792, 458 m/s). An obvious blue shift of the absorption edge is observed, indicating that the band gap of the β-SiC NWs is wider than that of bulk β-SiC. The band gap of the NWs, as calculated by Eq. (3), is about 2.666 eV.

4 Discussion

Band-gap widening in SiC nanomaterials due to the quantum confinement effect has been studied theoretically and experimentally [14, 27–29]. However, all of the previous studies focused on a size range of a few nanometers. Obviously, these studies cannot explain our experimental observations of band-gap widening in β-SiC NWs with diameters of up to hundreds of nanometers. As far as we know, nobody has studied the quantum confinement effect in NWs with large diameters, and some studies [15–17] attributed band-gap widening in large-diameter NWs to the quantum confinement effect without any explanation. We thought one plausible explanation would seem to be that the NWs are not made of a single crystal, but consist of nanocrystallites of a few nanometers in one dimension.

The first phenomenon we noticed was that the absorbance spectrum in Fig. 3 was persistently enhanced from 465 to 240 nm, which is defined as the intermediate zone in the figure. If the β-SiC NWs were single crystals, the zone should be very narrow, and the absorbance

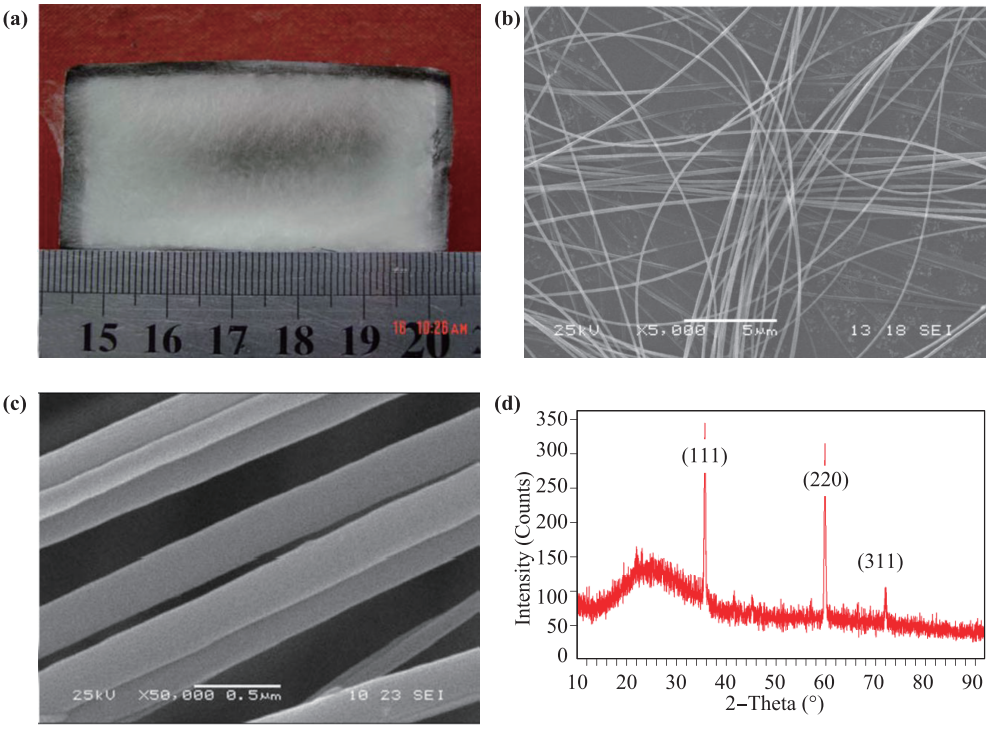

Fig. 2 **(a)** Morphology of white cotton-like products grown on the inner ceramic boats. **(b, c)** SEM morphology of the SiC NW arrays at different magnifications. **(d)** XRD pattern of the SiC NWs.

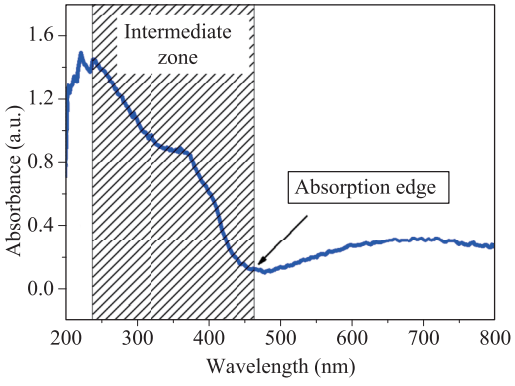

Fig. 2 UV-visible absorption spectrum of the SiC NWs. The intermediate zone, in which the absorbance was persistently enhanced, was defined as falling between 465 and 240 nm.

curve should be very steep. If we assume that the β-SiC NWs are made of nanocrystallites, according to Eqs. (2) and (3), the size of nanocrystallites should be 1.5–3.9 nm.

To explore the composition of the β-SiC NWs, a high-resolution transmission electron microscope (JEOL JEM-3010) with selected area electron diffraction (SAED) equipment was used, and TEM and HRTEM images of the SiC NWs are shown in Figs. 4(a)–(c). Figure 4(a) shows TEM images of the SiC NWs obtained at low temperature. The insets in Fig. 4(a) are HRTEM images of a typical NW at different magnifications. A black-and-white pattern with a period approximately 3 nm could be observed in the SiC NWs, and the boundary between the black and white patterns in the HRTEM image is shown in an inset of Fig. 4(a). The HRTEM image in the upper right inset in Fig. 4(a) shows a perfect crystal on both sides, and the lattice fringe spacing was measured to be 0.25 nm, which is consistent with the [111] plane space of β-SiC (JCPDS Card No. 73-1665). The SAED pattern [Fig. 4(b)] of the middle site of the white pattern showed a clear spot, indicating the single-crystal nature of this site. The SAED pattern could be indexed to β-SiC, and from the indexed spot, one could see that the NW was grown along the [111] direction. The same results were obtained for the middle site of the black pattern. However, there is an ambiguous layer with a thickness of approximately 0.5 nm between the black pattern and the white pattern shown in the upper right inset of Fig. 4(a). Apparently, the ambiguous layer is not a crystal phase and is most likely a defect layer, which is not a stacking fault or antiphase boundary, but a disordered amorphous phase. Now, it seems likely that the NW was not a single crystal, but was made up of nanosheets (black and white pattern) of β-SiC with thicknesses of approximately 3 nm. To perform a statistical analysis of the nanosheet thickness distribution using HRTEM, the four NWs labeled 1–4 in Fig. 4(c) were chosen, and the results are shown in Fig. 4(d). The nanosheet thickness distribution was within the range of 1–5 nm. A Gaussian fitting indicates that the maximal probability for the nanosheet thickness is about 2.7 nm,

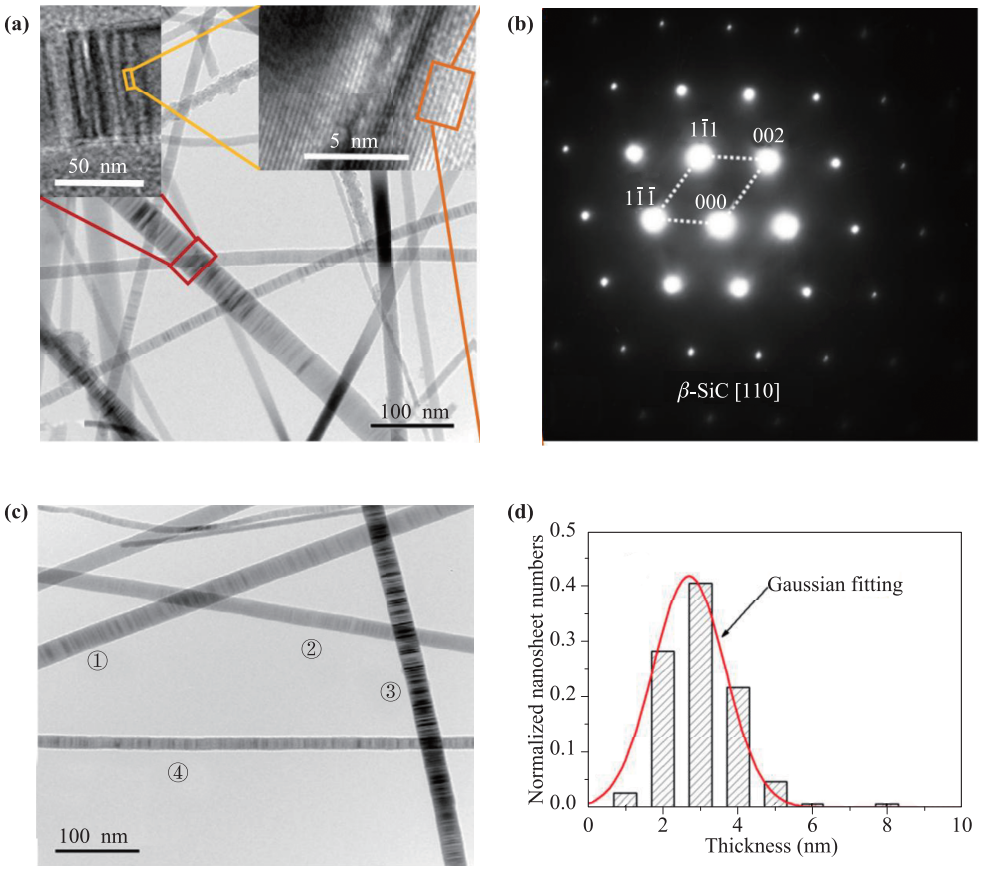

Fig. 4 **(a, c)** TEM images of SiC NWs obtained at low temperature. The insets in (a) are HRTEM images of a typical NW at different magnifications. **(b)** Corresponding indexed SAED pattern of the NWs, showing that the NWs were well crystallized, and the growth direction was [111]. **(d)** Distribution of normalized nanosheet number for four SiC NWs in (c) as function of nanosheet thickness with a center thickness size of 2.7 nm, which was obtained by a Gaussian fitting.

and the standard deviation is 0.94 nm. The results indicate that the probability of the nano-sheet thickness is 95% of the nanosheet thicknesses fall within plus or minus 1.96 times the standard deviation, i.e., from 0.86 to 4.54 nm.

Regarding the UV-visible absorption spectrum, if we ignore the influence of SiC nanosheets thicker than 4.54 nm, according to Eq. (2), the absorption edge of the UV-visible absorption spectrum for SiC NWs can be calculated as 2.561 eV. The value was close to 2.666 eV obtained from the experimental UV-visible absorption spectrum. However, there is an error of 0.105 eV compared with the experimental value. To analyze the cause of the error, we noticed two facts: i) the Coulomb term in Eq. (1) shifted E_g to lower energy (shown in Fig. 1 as a blue line), and ii) there are probably a large number of surface states in the crystal boundary between two nanosheets. These facts indicate that electrons or holes could be trapped or neutralized by surface states; consequently, Coulomb interaction has a weak effect on the band gap. If we omit the Coulomb term, we obtain

$$E_g \approx 2.30 + \frac{7.724}{d^2}. \quad (4)$$

Using this equation, the band gap for a nanosheet with a thickness of 4.54 nm could be calculated as 2.675 eV, which is very close to the experimental value of 2.666 eV; the difference is at an acceptable level.

5 Conclusion

In summary, to our knowledge, this was the first explicit observation of the quantum confinement effect in SiC NWs with diameters of up to hundreds of nanometers. A theoretical estimation indicated that only β-SiC NWs less than 6 nm in one dimension could exhibit an obvious band-gap widening effect, and the quantum confinement effect would widen the band gap as R^{-2}. HRTEM images of SiC NWs indicated that the β-SiC NWs consisted of nanosheets with thicknesses of 1–5 nm. Surface states at the boundary between nanosheets greatly decrease the influence Coulomb interaction of electrons and holes by trapping or neutralizing the carriers. This study could help to solve the discrepancy between the theory of quantum confinement, which indicates that band-gap widening occurs only at small sizes, and experimental observations of band-gap widening in large-diameter NWs, paving the way to new applications of the quantum confinement effect in nanoelectronics and optoelectronics.

Acknowledgements This work was supported by the National

Natural Science Foundation of China (Grant No. 61675234) and the Advanced Research Foundation of the National University of Defense Technology (Grant No. zk16-03-40).

References

1. L. Brus, Electronic wave functions in semiconductor clusters: Experiment and theory, *J. Phys. Chem.* 90(12), 2555 (1986)
2. L. Han, M. Zeman and A. H. M. Smets, Size control, quantum confinement, and oxidation kinetics of silicon nanocrystals synthesized at a high rate by expanding thermal plasma, *Appl. Phys. Lett.* 106(21), 213106 (2015)
3. L. Canham, Silicon quantum wire array fabrication by electrochemical and chemical dissolution of wafers, *Appl. Phys. Lett.* 57(10), 1046 (1990)
4. V. Lehmann and U. Gösele, Porous silicon formation: A quantum wire effect, *Appl. Phys. Lett.* 58(8), 856 (1991)
5. X. Wu, J. Fan, T. Qiu, X. Yang, G. Siu, and P. K. Chu, Experimental evidence for the quantum confinement effect in 3C-SiC nanocrystallites, *Phys. Rev. Lett.* 94(2), 026102 (2005)
6. F. Koch, V. Petrova-Koch, and T. Muschik, The luminescence of porous Si: The case for the surface state mechanism, *J. Lumin.* 57(1–6), 271 (1993)
7. Y. Kanemitsu, H. Uto, Y. Masumoto, T. Matsumoto, T. Futagi, and H. Mimura, Microstructure and optical properties of free-standing porous silicon films: Size dependence of absorption spectra in Si nanometer-sized crystallites, *Phys. Rev. B* 48(4), 2827 (1993)
8. D. Dai, X. Guo, and J. Fan, Identification of luminescent surface defect in SiC quantum dots, *Appl. Phys. Lett.* 106(5), 053115 (2015)
9. X. Wu, S. Xiong, G. Siu, G. Huang, Y. Mei, Z. Zhang, S. Deng, and C. Tan, Optical emission from excess Si defect centers in Si nanostructures, *Phys. Rev. Lett.* 91(15), 157402 (2003)
10. M. Cahay, Quantum confinement VI: Nanostructured materials and devices, Proceedings of the International Symposium, The Electrochemical Society, 2001
11. X. Wu, S. Xiong, D. Fan, Y. Gu, X. Bao, G. Siu, and M. Stokes, Stabilized electronic state and its luminescence at the surface of oxygen-passivated porous silicon, *Phys. Rev. B* 62(12), R7759 (2000)
12. T. W. Kim, C. H. Cho, B. H. Kim, and S. J. Park, Quantum confinement effect in crystalline silicon quantum dots in silicon nitride grown using SiH_4 and NH_3, *Appl. Phys. Lett.* 88(12), 123102 (2006)
13. S. W. Koch, Quantum Theory of the Optical and Electronic Properties of Semiconductors, World Scientific, 1994
14. S. Wang, C. Zhang, Z. Wang, and X. Zu, Quantum confinement effect in silicon carbide nanostructures: A first principles study, *Optoelectron. Rel. Mater* 4(6), 771 (2010)
15. S. Luo, J. Fan, W. Liu, M. Zhang, Z. Song, C. Lin, X. Wu, and P. K. Chu, Synthesis and low-temperature photoluminescence properties of SnO_2 nanowires and nanobelts, *Nanotechnology* 17(6), 1695 (2006)
16. V. Eskizeybek, A. Avcı, and M. Chhowalla, Structural and optical properties of CdO nanowires synthesized from $Cd(OH)_2$ precursors by calcination, *Cryst. Res. Technol.* 46(10), 1093 (2011)
17. A. Phuruangrat, P. Dumrongrojthanath, O. Yayapao, T. Thongtem, and S. Thongtem, Solvothermal synthesis and photocatalytic properties of CdS nanowires under UV and visible irradiation, *Mater. Sci. Semicond. Process.* 26, 329 (2014)
18. J. Y. Lee, X. Lu, and Q. Lin, High-Q silicon carbide photonic-crystal cavities, *Appl. Phys. Lett.* 106(4), 041106 (2015)
19. H. P. Phan, D. V. Dao, P. Tanner, L. Wang, N. T. Nguyen, Y. Zhu, and S. Dimitrijev, Fundamental piezoresistive coefficients of p-type single crystalline 3C-SiC, *Appl. Phys. Lett.* 104(11), 111905 (2014)
20. R. Shao, K. Zheng, Y. Zhang, Y. Li, Z. Zhang, and X. Han, Piezoresistance behaviors of ultra-strained SiC nanowires, *Appl. Phys. Lett.* 101(23), 233109 (2012)
21. H. P. Phan, The Piezoresistive Effect of Top Down p-Type 3C-SiC Nanowires, Springer International Publishing, 2017
22. D. Pandey and P. Krishna, The origin of polytype structures, *Progress in Crystal growth and Characterization*, **7**(1–4), 213 (1983)
23. G. Li, X. Li, Z. Chen, J. Wang, H. Wang, and R. Che, Large areas of centimeters-long SiC nanowires synthesized by pyrolysis of a polymer precursor by a CVD route, *J. Phys. Chem. C* 113(41), 17655 (2009)
24. G. Peng, Y. Zhou, Y. He, X. Yu, X. A. Zhang, G. Y. Li, and H. Haick, UV-induced SiC nanowire sensors, *J. Phys. D Appl. Phys.* 48(5), 055102 (2015)
25. G. Li, Ph. D. thesis, Synthesis and properties of ultralong SiC and Si3N4 nanowires, College of Science, National University of Defense Technology, China, 2010
26. G. Peng, Y. Zhou, Y. He, X. Yu, and G. Li, Fabrication and properties of ultraviolet photo-detectors based on SiC nanowires, *Sci. China Phys. Mech. Astron.* 55(7), 1168 (2012)
27. Y. Li, C. Chen, J. T. Li, Y. Yang, and Z. M. Lin, Surface charges and optical characteristic of colloidal cubic SiC nanocrystals, *Nanoscale Res. Lett.* 6(1), 454 (2011)
28. F. A. Reboredo, L. Pizzagalli, and G. Galli, Computational engineering of the stability and optical gaps of SiC quantum dots, *Nano Lett.* 4(5), 801 (2004)
29. A. M. Rossi, T. E. Murphy, and V. Reipa, Ultraviolet photoluminescence from 6H silicon carbide nanoparticles, *Appl. Phys. Lett.* 92(25), 253112 (2008)